# MINERAL
## DRESSING

# The Recovery of Rare-Earth Elements from Apatite Concentrate by Acid and Digestion-Water Leaching Processes in Morvarid Iron Mine, Iran

## A. Adib[a]*, R. Ahmadi[b], and E. Rahimi[a]

*[a]Islamic Azad University ,South Tehran Branch, Technical and Engineering Faculty,*
*Department of Mines and Petroleum, Tehran, 1584743311 Iran*
*\*e-mail: adib@azad.ac.ir*
*[b]Imam Khomeini International University (IKIU), Technical and Engineering Faculty, Mining Department,*
*Tehran, 1584743311, Iran*

**Abstract**—In this article, the recovery of the Y, La, Nd, and Ce rare-earth elements (REE) from apatite concentrate by acid leaching and digestion-water leaching processes were studied. The maximum REE recovery of 62% in the acid leaching process with sulfuric acid was obtained for La in the condition of 12 M acid concentration, leaching time of 4 h, process temperature of 25°C, and a liquid to solid ratio (L/S) of 1:5. In the optimal conditions in terms of process (220°C, 3 h and L/S (1:2)), the digesting process in the presence of sulfuric acid led to the recovery of La, Ce, Nd and Y at 93.92, 92.22, 92.04 and 91.00%, respectively. In contrast, the aqueous leaching process in the optimum conditions, including a leaching time of 5 h, at 80°C and L/S of 1:10 ended up recovering the La, Ce, Nd, and Y at 89.50, 88.45, 92.20 and 94.0%, respectively.

*Keywords:* Acid leaching, rare earth elements, effective parameters, digest-water leaching.

**DOI:** 10.1134/S1062739121010142

## INTRODUCTION

The Rare Erath Elements (REE) due to their unique spectroscopic properties have many applications in the production of important industrial materials [1–4].Thus, it is necessary to exploit indigenous resources and develop technologies to meet the future requirements by the recovery, separation and purification of REMs. Regarding the mentioned details, it is necessary to know the native resources and develop the appropriate recovery methods, separation, and purification of the rare earth elements.

Some minerals are investigated in the rare earth such as, monazite (phosphate mineral), bastnasite (fluorocarbonate mineral), allanite (hydrous silicate mineral), gadolinite (silicate of yttrium) and xenotime (phosphate of yttrium and their special application make profit in processing). Apatite is fluorophosphate calcium and a mineral concentrating on the REEs. Since the size of the ions of the REEs and the calcium ions are the same, the ions of the REEs are a good substitution for calcium ions in the apatite network [5]. The general formula of apatite is $Ca_{10}(PO_4)_6X_2$, which X is the ion flour with chlore and one hydroxyl group [6]. In average, apatite contains 0.1 to 0.8% of the oxides of the REEs [7]. REE ores are usually treated in two steps: physical concentration and leaching. The first step typically includes crushing the ore and physically separating the REOs from the ore. This separation process significantly increases the amount of REOs in the working material but is

successful only if the REEs are mostly concentrated in a single mineral phase such as a form of bastnäsite ($REECO_3F$) or monazite ($REEPO_4$) [8]. Unfortunately, this is not the case for the REE ore under research, which includes primarily apatite [$Ca_{10}(PO_4)_6(OH,F,Cl)_2$] as the significant source mineral. REEs in the apatite commonly occur as ionic substitutions for Ca within the crystal lattice rather than in discrete mineral form [9–11]. Intuitively, it is possible to recover REE concentrates by selective separation of REE-bearing apatite from the ore and it leads to the better economic condition [12]. The froth flotation is a typical process applied to phosphate ores. The gravity separation and magnetic separation were also found to be ineffective in concentrating REEs as the other physical concentration methods, but magnetic separation showed positive effects on impurity removal [13].

Sometimes ores containing rare earth elements are subjected to various pre-processing processes such as alkaline roasting to concentrate rare earth elements before refining operations. The product obtained from this process is then upgraded by various methods [14].

Leaching by acidic or alkaline reagents have used for the REEs extraction from ore. In the acid leaching, the Digestion method is usually used for the major REE minerals, including monazite, apatite, bastnäsite, and xenotime. In these methods, sulfuric acid has been added to REE concentrates in the temperature around 200°C. The obtained cake is leached with water to dissolve REEs [13]. Some investigation have been done on the leaching of REE in the acidic condition [15–20].

The results of these researches showed that apatite leached well in hydrochloric or nitric acid, but it was very difficult to attack with sulfuric acid unless the concentration and/or temperature were very high [20, 22, 23]. However, due to the complex metallurgy of REEs, a standard process for leaching REE-bearing minerals is not available. The choice of dissolution method depends on the mineralogy of the REE-containing phases and other non-REE minerals present in the ore, which often affect the effectiveness of the leaching operation. The current research aims to analyze the effect of nitric, sulfuric, and chloridric acids on the dissolution of the REEs in the apatite iron tailing of the processing plant of Morvarid mine, Zanjan. Moreover, this study will provide the analysis of the digestion method in the presence of sulfuric acid that followed by the water leaching of the iron pre-treatment apatite concentrate as well as the effective factors.

## 1. MATERIALS AND METHODS

The apatite concentrate obtained from the tailings sample of the Zanjan Morvarid iron ore processing plant, located in Iran with dimensions of $d_{80} = 75$ μm according to Fig. 1, was used to acid leaching and digestion-leaching process experiments. Sulfuric acid, nitric acid, and chloridric acid with a purity of 95, 65 and 37% (Merck), respectively, were used in both acid leaching and digestion-water leaching experiments. A double distilled water prepared by water distillation instrument (SDL 12l, OES Co., USA) was used in all experiments.

Field studies, petrography, ore microscopy, Electron MicroprobAnalysis, ICP-MS, XRD and XRF are examples of Tarom granitoid and mines in the SorkhehDizaj-Morvarid Zone. For these studies, more than 100 samples from different units were selected. In order to identify the chemical composition of minerals by EPMA, 20 samples of apatite and magnetite from these deposits were selected and analyzed.
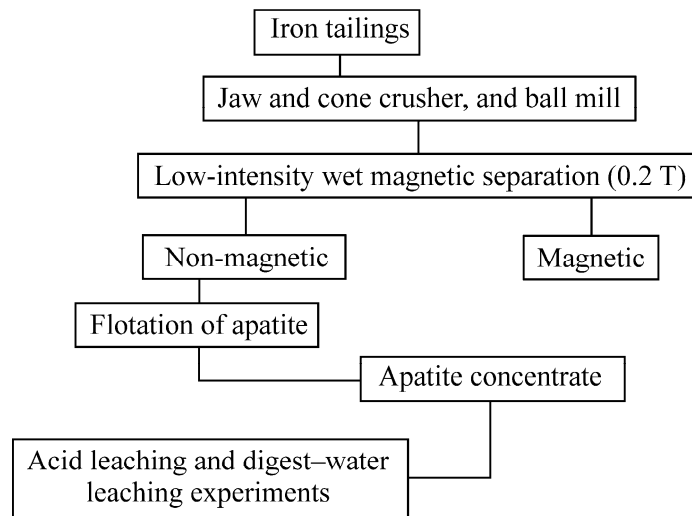
```
                        ┌──────────────┐
                        │ Iron tailings │
                        └──────────────┘
                ┌───────────────────────────────┐
                │ Jaw and cone crusher, and ball mill │
                └───────────────────────────────┘
        ┌──────────────────────────────────────────┐
        │ Low-intensity wet magnetic separation (0.2 T) │
        └──────────────────────────────────────────┘
        ┌──────────────┐            ┌──────────┐
        │ Non-magnetic │            │ Magnetic │
        └──────────────┘            └──────────┘
      ┌──────────────────┐
      │ Flotation of apatite │
      └──────────────────┘        ┌─────────────────────┐
                                   │ Apatite concentrate │
                                   └─────────────────────┘
    ┌────────────────────────────┐
    │ Acid leaching and digest–water │
    │     leaching experiments       │
    └────────────────────────────┘
```

**Fig. 1.** Flowsheet of the apatite concentrate preparation for acid leaching and digestion-water leaching experiments.

Apatite concentrate chemical analysis was performed using inductively coupled plasma optical emission spectrometry (ICP–OES, Perkin Elmer DRC-II quadrupole)) and X-ray fluorescence (Philips PW240, Netherland). The X-ray diffraction (XRD) pattern was obtained with a D/MAX 2200, Rigaku, Japan, X-ray diffractometer [21]. The XRF results are: show that the dominant compositions of the used concentrate are silica ($SiO_2$), $P_2O_5$, $Fe_2O_3$ and CaO (lc—loss in calcinations):

| $SiO_2$ | $Al_2O_3$ | CaO | MgO | $TiO_2$ | $SO_3$ |
|---------|-----------|-----|-----|---------|--------|
| 27.30 | 9.14 | 18.45 | 6.50 | 3.59 | 0.61 |
| $P_2O_5$ | $Na_2O$ | $K_2O$ | ZnO | CuO | MnO |
| 11.45 | 2.17 | 2.13 | 1.10 | 0.10 | 0.10 |
| $CeO_2$ | $La_2O_3$ | $Nd_2O_3$ | $Y_2O_3$ | $Fe_2O_3$ | lc |
| 1.75 | 0.63 | 1.61 | 0.84 | 11.51 | 0.97 |

The dominant compositions of the used concentrate are silica ($SiO_2$), $P_2O_5$, $Fe_2O_3$ and CaO. The ICP-OES results are:

| Rare earth element | $La_2O_3$ | $CeO_2$ | $Nd_2O_3$ | $Y_2O_3$ | Total |
|--------------------|-----------|---------|-----------|----------|-------|
| ppm | 6 510 | 17 400 | 16 250 | 8 430 | 48 590 |

The apatite concentrate contains 1.74% $CeO_2$, 0.63% $La_2O_3$, 1.61% $Nd_2O_3$ and 0.84% $Y_2O_3$). The concentrate is made of 4.86% rare earth oxides (La, Ce, Y and Nd). It suggests that the major mineral phases in the concentrate are apatite (consisting of La, Ce, Y and Nd compounds), quartz, calcite, magnetite and albite. Minor minerals were zeolite, phlogopite and pyrite, and so on.

Selected samples prepared in the Mineral Processing Research Center of Iran, in three dimensional fractions −300+150, −150+75 and −75 μm for mineralogical study (EPMA), degree of freedom, SEM analyses. The analysis of some unknown minerals was performed using Philips-Xpert Pro XRD machine on homogeneous powdered samples with dimensions of less than 60 microns and weighing between 2 and 10 grams. We have used Leo 1450 Vp Scanning Electron Microscope (SEM), and electron-probe microanalysis CAMECA EPMA (SX 100 model) to help identifying minerals by their composition (Tables 1 and 2; oxides are reported in wt. % and trace elements in ppm).

**Table 1.** Chemical composition of Tarom granitoid tailing samples (oxides are reported in wt. % and trace elements in ppm)

| Compound / element | Sample | | | | | | | | |
|---|---|---|---|---|---|---|---|---|---|
| | $W_3$ | $W_1$ | Ba | BaE | $BaE_2$ | $BaE_3$ | $W_4$ | $BaE_4$ | $Ba_1$ |
| $SiO_2$ | 70.24 | 70.21 | 69.27 | 70.13 | 69.34 | 60.98 | 61.40 | 65.08 | 63.15 |
| CaO | 2.20 | 2.15 | 2.60 | 2.30 | 2.97 | 5.96 | 5.25 | 2.65 | 5.00 |
| $Al_2O_3$ | 14.02 | 13.85 | 14.90 | 13.53 | 14.25 | 15.50 | 15.46 | 15.54 | 14.69 |
| $Fe_2O_3$ | 3.15 | 3.60 | 3.32 | 3.57 | 3.30 | 6.72 | 5.71 | 4.60 | 6.03 |
| MnO | 0.04 | 0.09 | 0.02 | 0.09 | 0.04 | 0.14 | 0.10 | 0.11 | 0.10 |
| MgO | 0.62 | 0.66 | 0.67 | 0.78 | 0.45 | 2.19 | 3.27 | 1.90 | 1.83 |
| $K_2O$ | 5.62 | 5.19 | 4.88 | 5.69 | 5.37 | 3.69 | 3.10 | 3.86 | 4.47 |
| $P_2O_5$ | 0.15 | 0.11 | 0.15 | 0.13 | 0.14 | 0.43 | 0.35 | 0.11 | 0.33 |
| $Na_2O$ | 3.25 | 3.28 | 3.52 | 3.05 | 3.46 | 3.26 | 4.64 | 5.00 | 3.31 |
| $TiO_2$ | 0.57 | 0.63 | 0.57 | 0.60 | 0.61 | 1.06 | 1.00 | 1.04 | 0.99 |
| Ba | 387.24 | 497.9 | 22.84 | 223.23 | 250.21 | 180.01 | 318.11 | 246.38 | 10.39 |
| Cs | 1.00 | 1.22 | 0.99 | 1.10 | 0.98 | 0.97 | 1.00 | 1.20 | 1.00 |
| Ce | 721.10 | 500.22 | 292.64 | 389.43 | 564.20 | 535.50 | 636.50 | 468.39 | 353.37 |
| Dy | 56.40 | 48.61 | 31.39 | 43.79 | 37.49 | 52.17 | 34.22 | 31.10 | 24.08 |
| Er | 20.50 | 25.63 | 16.36 | 23.83 | 19.81 | 28.11 | 18.42 | 16.42 | 13.03 |
| Eu | 6.23 | 9.25 | 4.81 | 7.55 | 6.45 | 6.93 | 5.95 | 5.02 | 3.35 |
| Gd | 81.94 | 63.87 | 37.51 | 55.69 | 49.07 | 63.30 | 45.75 | 38.52 | 29.97 |
| Ho | 10.90 | 15.57 | 9.94 | 14.36 | 11.78 | 17.58 | 11.14 | 10.53 | 8.02 |
| La | 321.82 | 229.16 | 132.53 | 174.17 | 243.28 | 227.99 | 288.51 | 214.24 | 156.91 |
| Lu | 2.80 | 3.25 | 2.42 | 3.31 | 2.52 | 4.00 | 2.28 | 2.40 | 1.84 |
| Nd | 482.19 | 412.95 | 214.44 | 329.07 | 308.04 | 363.7 | 310.32 | 227.86 | 170.2 |
| Pr | 123.20 | 175.74 | 90.76 | 136.00 | 126.71 | 143.65 | 132.84 | 95.97 | 70.97 |
| Sc | 23.34 | 26.10 | 12.88 | 31.53 | 22.52 | 24.39 | 25.99 | 33.77 | 12.59 |
| Sm | 91.43 | 85.00 | 47.46 | 71.66 | 65.57 | 82.41 | 63.45 | 49.60 | 38.25 |
| Tb | 11.53 | 15.34 | 9.44 | 13.64 | 11.81 | 16.13 | 11.41 | 9.87 | 7.60 |
| Th | 39.00 | 27.86 | 30.65 | 25.81 | 22.48 | 39.14 | 23.86 | 24.14 | 21.40 |
| Tm | 0.99 | 1.20 | 0.90 | 1.19 | 0.90 | 1.48 | 0.90 | 0.90 | 0.90 |
| U | 35.40 | 36.07 | 12.44 | 26.74 | 15.03 | 17.46 | 12.11 | 19.36 | 6.26 |
| Y | 288.00 | 283.29 | 186.95 | 254.83 | 207.33 | 305.49 | 184.83 | 171.57 | 141.29 |
| Rb | 32.84 | 136.77 | 10.00 | 32.56 | 71.57 | 24.66 | 61.50 | 50.54 | 12.00 |
| Nb | 60.87 | 74.47 | 29.11 | 30.29 | 10.75 | 32.99 | 29.28 | 29.64 | 23.80 |
| Sr | 142.80 | 140.08 | 46.65 | 77.18 | 111.36 | 107.50 | 130.07 | 145.05 | 36.69 |
| Yb | 14.84 | 13.18 | 9.25 | 12.63 | 10.21 | 15.39 | 9.80 | 9.00 | 6.98 |
| Ta | 1.01 | 1.05 | 1.00 | 0.99 | 1.00 | 1.00 | 1.00 | 0.99 | 1.00 |

**Table 2.** Chemical composition of Tarom granitoid concentrated samples (oxides are reported in wt. % and trace elements in ppm)

| Compound / element | Sample | | | |
|---|---|---|---|---|
| | 1 | 2 | 3 | 4 |
| $SiO_2$ | 63.62 | 64.73 | 64.50 | 64.30 |
| CaO | 4.81 | 3.61 | 3.69 | 4.52 |
| $Al_2O_3$ | 14.88 | 14.27 | 14.28 | 15.13 |
| $Fe_2O_3$ | 6.00 | 5.87 | 6.02 | 3.89 |
| MnO | 0.12 | 0.06 | 0.07 | 0.09 |
| MgO | 2.00 | 1.45 | 1.47 | 2.00 |
| $K_2O$ | 3.50 | 5.77 | 5.72 | 5.88 |
| $P_2O_5$ | 0.26 | 0.32 | 0.33 | 0.32 |
| $Na_2O$ | 3.79 | 2.95 | 2.95 | 2.94 |
| $TiO_2$ | 0.94 | 0.90 | 0.89 | 0.87 |
| Ba | 63.10 | 274.55 | 270.04 | 353.13 |
| Cs | 1.10 | 0.90 | 0.89 | 0.99 |
| Ce | 234.76 | 607.64 | 218.20 | 391.85 |
| Dy | 39.47 | 35.86 | 26.08 | 20.86 |
| Er | 19.15 | 19.40 | 14.58 | 10.92 |
| Eu | 3.61 | 5.96 | 2.96 | 3.05 |
| Gd | 43.15 | 50.39 | 32.64 | 26.43 |
| Ho | 12.66 | 11.60 | 8.73 | 6.90 |
| La | 98.41 | 277.14 | 92.06 | 177.40 |
| Lu | 3.09 | 2.41 | 2.24 | 1.61 |
| Nd | 217.31 | 352.86 | 173.82 | 167.09 |
| Pr | 86.22 | 155.17 | 70.50 | 71.05 |
| Sc | 8.42 | 12.57 | 9.07 | 20.41 |
| Sm | 52.92 | 69.63 | 40.37 | 35.43 |
| Tb | 11.04 | 11.92 | 8.68 | 6.55 |
| Th | 31.27 | 33.46 | 29.49 | 18.70 |
| Tm | 1.14 | 0.90 | 0.90 | 0.90 |
| U | 8.37 | 21.22 | 7.08 | 15.84 |
| Y | 235.47 | 208.27 | 168.31 | 115.07 |
| Rb | 72.20 | 39.20 | 23.42 | 49.05 |
| Nb | 52.68 | 26.78 | 13.25 | 28.11 |
| Sr | 43.84 | 139.89 | 101.19 | 153.34 |
| Yb | 11.19 | 9.90 | 8.56 | 6.14 |
| Ta | 0.98 | 0.97 | 0.99 | 0.96 |

The apatite concentrate was divided into homogeneous, small size fractions using a riffle separator. The sample was wet screened to produce three size fractions of –300+150, –150+75 and –75 μm. Microscopic mineralogical studies were performed on thin and polished sections of the concentrate sample to identify the major and minor minerals and also to determine the degrees of freedom of the minerals by ZEISS Axioplan 2 polarizing light microscope with reflection and cross light. Also, EPMA studies were performed with the CAMECA SX 100 electron microprobe analyzer to identify

minerals containing rare elements over the mentioned dimensional ranges. According to the mineralogical studies, the major minerals (more than 10%) include quartz, apatite, calcite, magnetite and albite and accessory minerals (between 2–10%) including phlogopite, zeolite, chlorite, hematite and pyrite and minor minerals (less than 2% (chalcopyrite, covellite, sphalerite, lepidocrocite, goethite, and monazite) were identified.

Figure 2 shows the main and minor minerals of the concentrate sample. According to the degrees of freedom studies on polished sections in the ranges of –300+150, –150+75 and –75 μm, apatite minerals have degrees of freedom of 55, 75 and 82%, respectively. The main mineral contains the rare earth elements is the apatite. However, rare earth elements were also found in magnetite and quartz minerals in minor amounts. These minerals have various size ranges from 5 to 100 μm.

Basic leaching tests were done by using distilled water and the ranges of 0.1–12.0 M for sulfuric acid and 0.5–3.0 M for hydrochloric and nitric acid. All of the leaching tests were replicated three times, and average values obtained after removing significant outliers were used for analysis. Fifty grams of the pretreated-sample were added to a beaker containing 200 mL of the acid solution at pH 1. In the next step, the slurry was agitated with an impeller-type stirrer. To stabilize temperature and prevent evaporation an aluminum foil used the beaker during the test. When the pulp height is diminished, a specific amount of distilled water was added. The solution samples were gathered at regular time intervals and the solid particles was separated from the leachate using a filter for lower acid conditions (0.1–2.0 M acids) or a centrifuge for higher acid conditions (5.0–13.0 M acids). The solution was separated and diluted with 1.0 M hydrochloric acid to prevent precipitation of REEs and analyzed using an inductively coupled plasma optical emission spectrometer.

The apatite concentrate grind and situate in acidic digestion using sulfuric acid. The digested mass which made in the digestion step (sulfate cake containing REEs) was leached with distilled water by filtration. In order to studies the optimum conditions of the digestion step, a certain amount of sulfuric acid was heated in a Pyrex beaker on a heater.

In specific temperature, the apatite concentrate was added to the sulfuric acid in the beaker with the amount of five grams and mechanical stirrer agitated the mixture for a specific time. Then, the digested sample was left in the air until dried, and a "dry gray solid residue" or the digested mass was obtained. Afterward, the digested mass was re-leached with distilled water. The leaching experiments were performed in a batch Pyrex reactor and a hot-plate with a magnetic stirrer agitated the suspension at a predetermined temperature. Five grams of the digested mass (produced in the digestion stage) were transferred into a specific amount of distilled water. Then, the leach liquor was filtered with a centrifuge, and finally, the leach liquor and the precipitate were analyzed with IC-Mass.
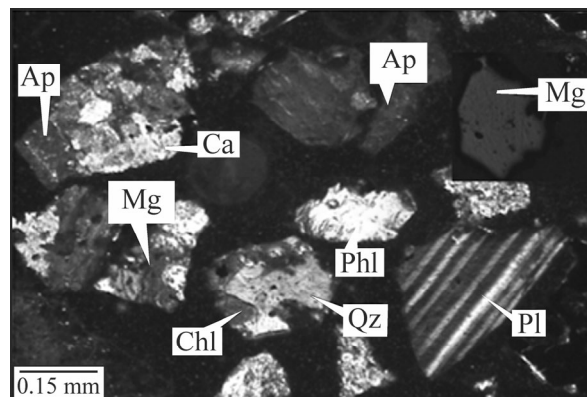


**Fig. 2.** Apatite (Ap), calcite (Ca), magnetite (Mg), quartz (Qz), albite (Pl), phlogopite (Phl); chlorite (Chi) minerals as major minerals in dimensional range ($d_{80}$ = 75 μm).

## 2. RESULTS AND DISCUSSION

The granitoid are classified into 5 types, I, S, M, A and H based on petrological and geochemical features and characteristics. Granitoid samples and the rocks containing apatite in Sorkheh Dizaj, Aliabad, Morvarid and Zaker mines were analyzed by ICP–MS method. As previously mentioned, the Tarom area granitoid are type I, this type of granite [22, 23] are Meta-Aluminous, containing Hornblende, Biotite and small amounts of pyroxene, magnetite + sphene, ilmenite, alkali feldspar and microgranular enclaves contain hornblende. Aluminum saturation index (ASI) in granitoid represents rock chemistry and related mineralogy. The samples studied in the Aluminum Saturation Index diagram [24] and have a meta-aluminous nature (Fig. 3).

In this section, using chemical analysis data, first determine the position of granitoid rocks in petrological diagrams, and then investigate the variations of major and trace elements in them and also compare them with the analytical data of concentrate and gang samples. In relation to the chemical classification of the intrusive rocks in TAS diagrams Cox et al., and Middlemost [25, 26] show that these samples range from diorite, monzodiorite, gabbro diorite, tailings samples range from granite to quartz diorite (granodiorite), monzonite, quartz monzonite, and concentrated samples in the granodiorite to quartz monzonite range.

In the Debon and Lefort diagram [27], intrusive mass samples are in the quartz diorite, tonalite, and quartz monzodiorite, gang samples in the quartz monzodiorite, quartz monzonite, and concentrated samples quartz monzodiorite, and the quartz syenite, occur.

The results show the change in the leaching efficiency with the sulfuric acid concentration. The experiments were run for 1 h at 25°C. When the acid concentration increased the acid concentration is increased at low acid concentrations, too. However, the leaching level decreased at 4.0 M. This may result from re-precipitation of REEs via calcium sulfate formation. It is obvious that calcium sulfate hydrates (gypsum, hemihydrate, and anhydrite) are readily formed wherever calcium and sulfate are present together in aqueous solutions [28].

The residue after leaching shows the presence of Gypsum ($CaSO_4 \cdot 2H_2O$) and Anhydrite ($CaSO_4$) as the results of the XRD analyses. This residue may contain REEs by isomorphs substitutions for $Ca^{2+}$ [29], because Ca and REEs have similar ionic radius.

The variations in the leaching levels in the different times have been shown in the Fig. 4 when 12.0 M sulfuric acid was used as the leaching agent. It can be also seen that increasing the leaching time from 1 to 4 hours, leaching recovery increased with a high slope. By increasing the time to 6 hours, the leaching reaction reaches equilibrium. Despite high concentrations of sulfuric acid (12 M) and leaching time of 6 hours, high recovery has not been achieved for the leaching process. The maximum recovery is for La with about 62 percent.
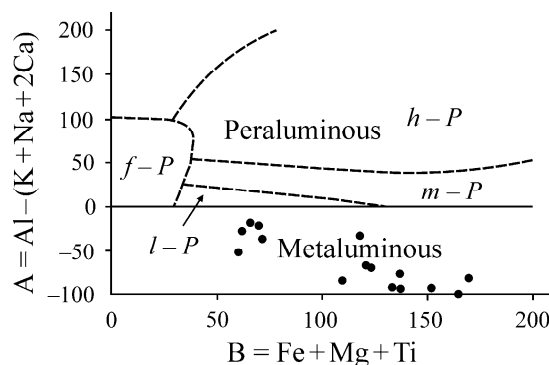


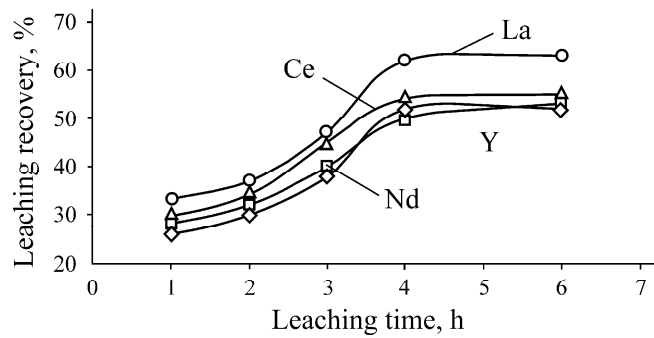**Fig. 3.** The position of the Tarom granitoid rocks on the diagram [24].

**Fig. 4.** Change in leaching levels with time using sulfuric acid at 25°C. Initial acid concentration: 12.0 M; L/S ratio: 5:1.

Meantime, the total soluble Ca material varies with the sulfuric acid concentration in a pattern very similar to the leaching pattern. This result suggests that sulfuric acid may not be a suitable leaching agent for this ore, as the side reaction, Ca(REE) sulfate precipitation, limits the REE leaching level, which did not exceed 62%, even when a significant excess of acid (12.0 M) and time leaching of 6 h was used. Also, a very high concentration of high soluble Ca species, which would undoubtedly cause complications during REE recovery by either precipitation or solvent extraction.

The use of sulfuric acid in leaching process of eudialyte has also been shown by researchers that sulfuric acid, which ensures the highest extraction of Zr and rare earth metals in pregnant solution, contributes to maximum formation of silica gel and considerable quantity of gypsum and insoluble sulfates, which results in high loss of Zr and rare earth metals. The use of nitric and chlorohydric acids reduces the loss of Zr and rare earth metals by 2–5 times [11].

Figure 5 shows the variation in the leaching levels with the initial concentration of hydrochloric acid. Almost no REEs were leached when the concentration was less than 1.0 M. At higher concentrations of hydrochloric acid, the leaching levels increased sharply. At an acid concentration of 3.0 M, nearly 90% of the REEs were leached. However, the amount of Ca in the leachate was also very high.

Variation in the leaching recovery with different concentrations is shown Fig. 6. No REEs, aside from Y, were leached at 1 M, whereas impurities such as P and Ca were leached quite well. However, about 90% of the REEs were leached, when the acid concentration was increased to 3.0 M. Results of these experiments similar to the hydrochloric acid case. Since nitric acid is generally more expensive than hydrochloric acid, it was not considered in later tests. Therefore, hydrochloric acid was chosen as the optimum leaching agent for this apatite REE ore.
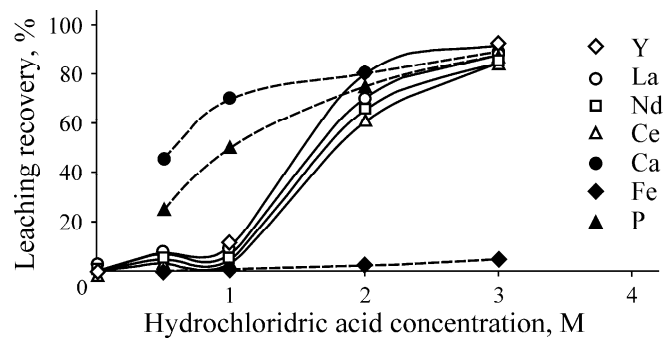


**Fig. 5.** Leaching levels at various initial sulfuric acid concentrations at 25°C, leaching time: 2.5 h, L/S ratio: 5:1.
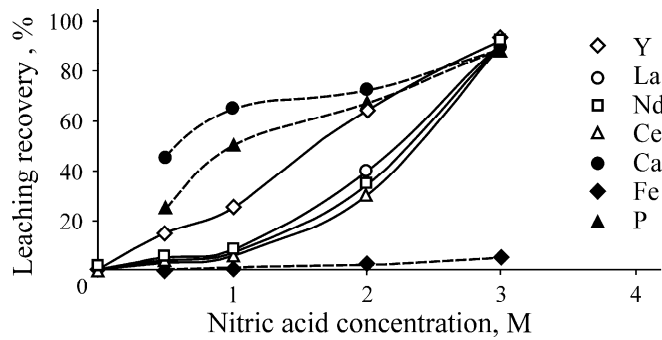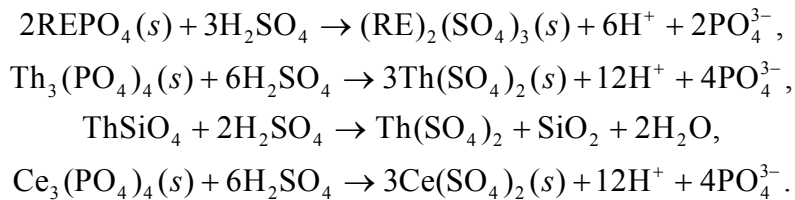
**Fig. 6.** Leaching levels at various initial nitric acid concentrations at 25°C, leaching time: 2.5 h, L/S ratio:5:1).

Figure 7 shows the effect of digestion process temperature on the recovery of rare elements from apatite concentrate with constant conditions of 3 hours and solid to liquid ratio of 1.75. Apatite lattice is not soluble in water because of strong bonds between REEs and oxygen. In the acidic digestion process, these strong bindings are broken, and soluble REEs' sulfates are formed. The following reactions occur during the digestion process [30]:

$$2REPO_4(s) + 3H_2SO_4 \rightarrow (RE)_2(SO_4)_3(s) + 6H^+ + 2PO_4^{3-},$$

$$Th_3(PO_4)_4(s) + 6H_2SO_4 \rightarrow 3Th(SO_4)_2(s) + 12H^+ + 4PO_4^{3-},$$

$$ThSiO_4 + 2H_2SO_4 \rightarrow Th(SO_4)_2 + SiO_2 + 2H_2O,$$

$$Ce_3(PO_4)_4(s) + 6H_2SO_4 \rightarrow 3Ce(SO_4)_2(s) + 12H^+ + 4PO_4^{3-}.$$

The results showed that, the temperature effect on the digestion process is negative. There are some reasons for the negative effect of temperature on the digestion process. There are some reasons for the negative effect of temperature on the digestion process, which mentioned in the following.

In Fig. 7, it is obvious that increasing the temperature can lead to low recovery of the digestion process. There is so many reasons for that.

First, as mentioned in the research literature, the digested residue should not be dried completely, since the formation of insoluble compounds increases in higher temperatures which will decrease digestion recovery [30, 31]. One of the reasons of low recovery is increase the amount of the insoluble compounds. Second, because the digestion step is not conducted in the vacuum, and the system is exposed to the air, increasing the temperature increases the sulfuric acid evaporation rate. Therefore, the contact time (reaction time) between liquid (sulfuric acid) and solid (apatite concentrate) decreases.
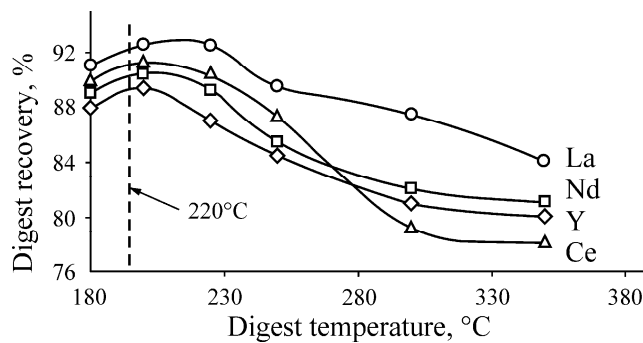


**Fig. 7.** The effect of digestion process temperature on the recovery of the rare elements from apatite concentrate with constant conditions of 3 hours for time and solid to liquid ratio of 1.75.

The results of the recovery of the rare elements with constant conditions of 220°C and 3 hours in a different liquid to solid ratios. Regard to the figure by increasing the, the recovery of all rare elements in the digestion stage is increased. In this figure can be seen that increasing in the L/S ratio from 0.5 to 2, lead to recovery of the REE minerals to 90 percents. With a further increase in the ratio to above 2, recovery does not significantly change.when the L/S ratio increase, improves the recovery of the rare earth as the possibility of effective contacts between the solid and liquid and that is why of the presence of extra acid in the reaction medium. The optimum condition in the digestion process is proposed to be: temperature of 220°C, time of 3 hours and the L/S ratio of 2.0. This optimum condition used to produce a dry gray solid residue, which was the feed in the leaching experiments.

As the results of the reactions, it can be found that the dry gray digested mass mostly consists of sulfate salts of REEs and REES sulfates, dissolved in the water, in the leaching step. However, some impurities and unreacted apatite, which consists of REEs phosphates and also insoluble compounds that were made in the digestion process, remain as a precipitate. The following reactions occur in the leaching step [31]:

$$(RE)_2(SO_4)_3 nH_2O(s) \rightarrow 2RE^{3+} + 3SO_4^{-2} + nH_2O,$$

$$Th(SO_4)_2(s) \rightarrow Th^{4+} + 2SO_4^{2-},$$

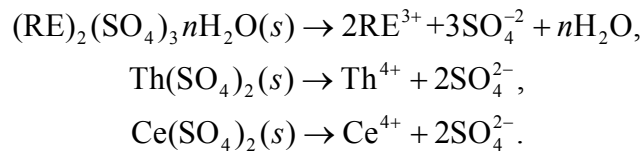$$Ce(SO_4)_2(s) \rightarrow Ce^{4+} + 2SO_4^{2-}.$$

Figure 8 shows the effect of aqueous leaching time on leaching recovery with constant conditions L/S = 5 and 25°C. According to the figure, the highest recovery of the rare earth elements for La, Ce, Nd and Y was 55.50, 54.45, 58.20 and 60%, respectively, in 5 hours. The highest rate of recovery of rare earth elements for La, Ce, Nd and Y was 84.0, 83.50, 54.35 and 86.0 at 80°C, respectively.

Figure 9 shows the effect of the L/S ratio on leaching recovery with constant conditions of 5 hours leaching time and temperature of 80°C. The highest rate of recovery of rare earth elements for La, Ce, Nd and Y was obtained 89.50, 88.45, 92.20 and 94.0%, respectively, at L/S = 10. When the L/S ratio increase, the recovery of the rare earth increase, too, as a result of increasing the solid and liquid interfaces, where the reaction between solid and liquid is expected to occur. The disruption of the solid product occurs while leaching, and the new interfaces need more liquid to react. Also, increasing the L/S ratio causes the solution to become saturated later, and these all increase the leaching recovery [32, 33]. Therefore, according to the results, with optimum aqueous leaching condition which is including 5 h time, 80°C and L/S of 10, the highest recovery of rare earth elements from digest solid for La, Ce, Nd and Y 89.50, 88.45, 92.20 and 94.0% were obtained, respectively.
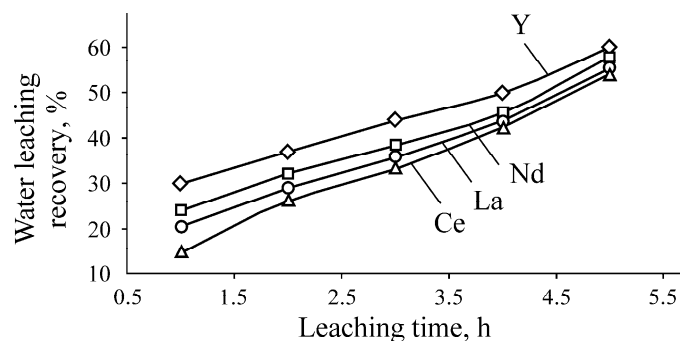


**Fig. 8.** Effect of aqueous leaching time on leaching recovery with constant conditions L/S = 5 and 25°C.
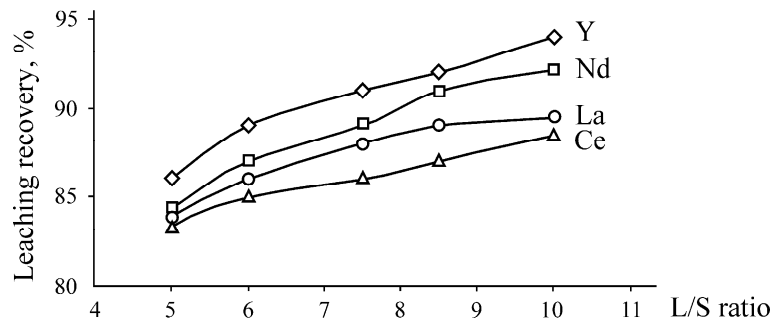
**Fig. 9.** Effect of L/S ratio on the recovery of aqueous leaching with constant conditions of 80°C and 5 hours.

CONCLUSIONS

According to petrography, and geochemical data, samples of the Tarom intrusive masses (Sorkheh-Dizaj Mines, Zanjan), are diorite, monzodiorite, quartz monzodiorite and rarely granodiorite, tonalite, quartz diorite and quartz monzodiorite, gang samples are monzonite, quartz monzodiorite, granodiorite, monzodiorite, and concentrate samples range of quartz monzonite, quartz monzodiorite, tonalite, and quartz syenite. The apatite specimens are in the range of Kyruna-type deposits. Iron–apatite ore contains chemical elements such as Ce La, Nd and Y along with monazite ore, and of course many more minerals including magnetite, apatite, hematite, quartz, feldspar, and etc.

Magnetite-apatite mineralization of this region is the result of the magmatic decomposition of an alkaline magma rich in REEs such as Th and U, as well as elements such as cl and F resulting from the partial melting of the upper mantle. Based on geochemical data, the geotechnical environment of the rocks studied pre plate collision, and is less related to post collision uplift. Tarom granitoid specimens are in the range of volcanic arc granitoid (VAG), as well as volcanic arc granitoid and collision granitoid (VAG+syn+COLG). The placement of some gangs and concentrate samples in the ORG and WPG ranges is due to changes in trace elements during transformations and alterations due to the infiltration of hydrothermal solutions into the intrusive mass. Based on chondrite normalized REEs of Tarom granitoid masses (Sun and McDonough, 1989), in concentrates and gangs, enrichment of LREEs such as La, Ce, Pr and HREEs including Tm, Yb and Lu.

In this research, acid leaching and aqueous digestion-leaching experiments by using the sulfuric acid, hydrochloric acid, and nitric acid, were performed on the apatite concentrate obtained from iron tailings. Based on ICP analysis results the apatite concentrate is made of 4.86% rare earth oxides (La, Ce, Y and Nd). According to mineralogical studies, the major minerals were quartz, apatite, calcite, magnetite, and albite. Degrees of freedom studies on the polished sections in the range of −150+100, −150+75 and −75 micron showed that apatite has degrees of freedom of 55, 75 and 82%, respectively. According to EPMA studies, the acid leaching experiments performed by sulfuric acid showed that by increasing the acid concentration up to 2 M, recovery of the rare elements increased. Although further increasing the acid concentration up to 4 M due to the formation of hydrated calcium sulfate, which is an insoluble compound and containing rare elements, the recovery decreased. The highest rare elements recovery in acid leaching with sulfuric acid with the optimum conditions was about 62%. The results of leaching experiments in the presence of hydrochloric acid and nitric acid showed that with optimum conditions of 25°C, 2.5 h leaching time, L/S ratio of 5:1 and 3 M acid sulfuric, recovery of the Y, La, Nd and Ce reached about 90%. Digestion process in the presence of sulfuric acid with optimum conditions of 220°C, 3 h time, and L/S ratio of 2.0 recovery of

La, Ce, Nd and Y was 93.92, 92.22, 92.04 and 91.00%, respectively. The results also showed that in the optimum conditions of aqueous leaching on the gray solid of the digestion process, with 5 h time, 80°C and liquid to solid ratio of 10, the highest recovery of La, Ce, Nd and Y was 89.50, 88.45, 92.20 and 94.0%, respectively.

## REFERENCES

1. Kim, E. and Osseo-Asare, K., Aqueous Stability of Thorium and Rare Earth Metals in Monazite Hydrometallurgy: $Eh-pH$ Diagrams for the Systems $Th^-$, $Ce^-$, $La^-$, $Nd^-$ $(PO_4)-(SO_4)-H_2O$ at 25°C, *Hydrometallurgy*, 2012, vol. 113–114, pp. 67–78.

2. Kim, E., Bae, I., Chai, S., and Shin, H., Mechanochemical Decomposition of Monazite to Assist the Extraction of Rare Earth Elements, *J. of Alloys and Compounds*, 2009, vol. 486, no. 1–2, pp. 610–614.

3. *Rare Element*, Resources Ltd., News Releases, 2011.

4. http://www.lighting.philips.com/pwc_li/us_en/lightcommunity/trends/phosphor/assets/philips_REO_Brochure_P-6281.pdf.

5. Gupta, C. and Krishnamurthy, N., *Extractive Metallurgy of Rare Earths*, New York: CRC Press, 2004.

6. Preston, J.S., Cole, P.M., Craig, W.M., and Feather, A.M., The Recovery of Rare Earth Oxides from a Phosphoric Acid by Product. Part 1: Leaching of Rare Earth Values and Recovery of a Mixed Rare Earth Oxide by Solvent Extraction, *Hydrometallurgy*, 1996, vol. 41, no. 1, pp. 1–19.

7. Habashi, F., Extractive Metallurgy of Rare Earths, *Can. Metall. Q.*, 2013, vol. 52, no. 3, pp. 224–233.

8. Chi, R., Tian, J., Zhu, G., Wu, Y., Li, S., Wang, C., and Zhou, Z.A., Kinetics of Rare Earth Leaching from a Manganese-Removed Weathered Rare-Earth Mud in Hydrochloric Acid Solutions, *Separ. Sci. Technol.*, 2006, vol. 41, pp. 1099–1113.

9. Zielinski, S., Szczepanik, A., and Buca, B., Recovery of Lanthanides from Kola Apatite in Phosphoric Acid Manufacture, *J. Chem. Technol. Biotechnol.*, 1993, vol. 56, pp. 355–360.

10. Martin, P., Carlot, G., Chevalier, A., Den-Auwer, C., and Panczer, G., Mechanisms Involved in Thermal Diffusion of Rare Earth Elements in Apatite, *J. Nucl. Mater.*, 1999, vol. 275, pp. 268–276.

11. Chanturia, V.A., Minenko, V.G., Koporulina, E.V., Ryazantseva, M.V., and Samusev, A.L., Influence of Acids on Extraction Efficiency of Zirconium and Rare Earth Metals in Eudialyte Concentrate Leaching, *J. Min. Sci.*, 2019, vol. 55, no. 6, pp. 984–994.

12. Razmyslov, I.N., Kotova, O.B., Silaev, V.I., Rostovtsev, V.I., Kiseleva, D.V., Kondrat'ev, S.A., Microphase Heterogenization of High-Iron Bauxite as a Result of Thermal Radiation, *J. Min. Sci.*, 2019, vol. 55, no. 5, pp. 811–823.

13. Kim, R., Cho, H., Han, K.N., Kim, K., and Mun, M., Optimization of Acid Leaching of Rare-Earth Elements from Mongolian Apatite-Based Ore, *Minerals*, 2016, vol. 63, no. 6, pp. 1–15.

14. Purwanti, T., Setyadji, M., Astuti, W., Perdana, I., and Tri Bayu Murti Petrus, H., Phosphate Decomposition by Alkaline Roasting to Concentrate Rare Earth Elements from Monazite of Bangka Island, Indonesia, *J. Min. Sci.*, 2020, vol. 56, pp. 477–485.

15. Jorjani, E., Bagherieh, A.H., and Chelgani, S.C., Rare Earth Elements Leaching from Chadormalu Apatite Concentrate: Laboratory Studies and Regression Predictions, *Korean J. Chem. Eng.*, 2011, vol. 28, pp. 557–562.

16. Aly, M.M. and Mohammed, N.A., Recovery of Lanthanides from Abu Tartur Phosphate Rock, *Egypt. Hydrometallurgy*, 1999, vol. 52, pp. 199–206.

17. Sandström, A. and Fredriksson, A., Apatite for Extraction—Leaching of Kiirunavaara Apatite for Simultaneous Production of Fertilizers and REE, *Proc. of the 26th Int. Miner. Proces. Congress, IMPC-2012, Innovative Proc. for Sustainable Growth*, New Delhi, India, 2012, pp. 4707–4714.

18. Pereira, F. and Bilal, E., Phosphoric Acid Extraction and Rare Earth Recovery from Apatites of the Brazilian Phosphatic Ores, *Romanian J. Mineral. Depos.*, 2012, vol. 85, pp. 49–52.

19. Habashi, F., The Recovery of the Lanthanides from Phosphate Rock, *J. Chem. Technol. Biotechnol. Chem. Technol.*, 1985, vol. 35, pp. 5–14.

20. Chanturia, V.A., Koporulina, E.V., Minenko, V.G., and Samusev, A.L., Energy Effects on Structural and Chemical Transformations of Base Minerals of Eudialyte Concentrate in Nitric Acid Leaching, *J. Min. Sci.*, 2019, vol. 55, no. 4, pp. 634–642.

21. Chanturia, V.A., Bunin, I.Zh., Ryazantseva, M.V., Chanturia, E.L., Samusev, A.L., Koporulina, E.V., and Anashkina, N.E., Intensification of Eudialyte Concentrate Leaching by Nanosecond High-Voltage Pulses, *J. Min. Sci.*, 2018, vol. 54, no. 4, pp. 646–655.

22. Chappell, B.W. and White, A.J.R., I- and S-Type Granites in the Lachlan Fold Belt, *Transactions of the Royal Society of Edinburgh, Earth Sci.*, 1992, vol. 83, pp. 1–26.

23. Kanen, R., *Distinguishing between S- and I-Type Granites*, Minerals Services, Melbourne, Australia, 2001.

24. Villaseca, C., Barbero, L., and Herreros, V., A Re-Examination of the Typology of Peraluminous Granite Types in Intracontinental Orogenic Belts, *Trans. R. Soc. Edinb., Earth Sci.*, 1998, vol. 89, pp. 113–119.

25. Cox, K.G., Bell, J.D., and Pankhurst, R.J., *The Interpretation of Igneous Rocks*, George, Allen and Unwin, London, 1979.

26. Middlemost, E.A., K. *Magmas and Magmatic Rocks. An Introduction to Igneous Petrology*, Longman, London, 1994.

27. Debon, F. and Le Fort, P., A Cationic Classification of Common Plutonic Rocks and Their Magmatic Associations: Principles, Method, Applications, *Bulletin de Minéralogie*, 1988, vol. 111, pp. 493–510.

28. El-Nadi, Y., El-Hefny, N.E., and Aly, H.F., Solvent Extraction and Recovery of Y(III) and Yb(III) from Fluorspar Mineral, *Int. J. of Minerals, Metall. and Mater.*, 2013, vol. 20, pp. 713–719.

29. Azimi, G. and Papangelakis, V.G., The Solubility of Gypsum and Anhydrite in Simulated Laterite Pressure Acid Leach Solutions up to 250°C, *Hydrometallurgy*, 2010, vol. 102, pp. 1–13.

30. Wang, L., Long, Z., Huang, X., Yu, Y., Cui, D., and Zhang, G., Recovery of Rare Earths from Wet-Process Phosphoric Acid, *Hydrometallurgy*, 2010, vol. 101, pp. 41–47.

31. Gupta, C.K., *Hydrometallurgy in Extraction Processes*, Wiley-VCH, 1990.

32. Hu, Z. and Qi, L., *Sample Digestion Methods*, Elsevier Ltd., 2014, pp. 87–109.

33. Kumari, A., Panda, R., Jha, M.K., Lee, J.Y., Kumar, J.R., and Kumar, V., Thermal Treatment for the Separation of Phosphate and Recovery of Rare Earth Metals (REMs) from Korean Monazite, *J. of Industrial and Eng. Chemistry*, 2014, vol. 21, pp. 696–703.